AGU PUBLICATIONS

Geophysical Research Letters

RESEARCH LETTER
10.1002/2015GL065704

Key Points:
- Ice is still quite thick in Northwest Passage and potentially hazardous for shipping
- Mean ice thickness depends on age and specific source region of sea ice in previous summers
- Mean ice thickness and deformation decrease with decreasing northern latitude

Supporting Information:
- Supporting Information S1
- Data Set S1
- Data Set S2
- Data Set S3

Correspondence to:
C. Haas,
haasc@yorku.ca

Citation:
Haas, C., and S. E. L. Howell (2015), Ice thickness in the Northwest Passage, *Geophys. Res. Lett.*, *42*, 7673–7680, doi:10.1002/2015GL065704.

Received 6 AUG 2015
Accepted 31 AUG 2015
Accepted article online 4 SEP 2015
Published online 25 SEP 2015

Ice thickness in the Northwest Passage

Christian Haas[1,2] and Stephen E. L. Howell[3]

[1]Department of Earth and Space Sciences and Engineering, York University, Toronto, Ontario, Canada, [2]Formerly at Department of Earth and Atmospheric Sciences, University of Alberta, Edmonton, Alberta, Canada, [3]Climate Research Division, Environment Canada, Toronto, Ontario, Canada

Abstract Recently, the feasibility of commercial shipping in the ice-prone Northwest Passage (NWP) has attracted a lot of attention. However, very little ice thickness information actually exists. We present results of the first ever airborne electromagnetic ice thickness surveys over the NWP carried out in April and May 2011 and 2015 over first-year and multiyear ice. These show modal thicknesses between 1.8 and 2.0 m in all regions. Mean thicknesses over 3 m and thick, deformed ice were observed over some multiyear ice regimes shown to originate from the Arctic Ocean. Thick ice features more than 100 m wide and thicker than 4 m occurred frequently. Results indicate that even in today's climate, ice conditions must still be considered severe. These results have important implications for the prediction of ice breakup and summer ice conditions, and the assessment of sea ice hazards during the summer shipping season.

1. Introduction

The fabled Northwest Passage (NWP) is a system of gulfs, straits, sounds, and channels in the Canadian Arctic Archipelago (CAA) connecting the Beaufort Sea in the west with Baffin Bay in the east (Figure 1, inset). It presents a potential Arctic shipping route between markets in the northern Pacific and Atlantic regions which is much shorter than routes through the Panama or Suez Canals. The NWP is an alternative route to the Northern Sea Route (NSR) along the coast of Siberia [e.g., *Smith and Stephenson*, 2013]. Both the NWP and NSR are covered by drifting or landfast sea ice for most of the year, which forms a navigational obstacle even for ice-breaking ships and a safety hazard for less capable ships. The NSR is characterized by the presence of predominantly thin drifting first-year ice (FYI) and has been ice free for several weeks during recent summers. However, in winter the waters of the NWP are largely covered by thick landfast FYI which is interspersed with fields of landfast multiyear ice (MYI) having survived one or several preceding summers. Although most FYI in the NWP melts during summer, some may survive to form locally derived MYI [*Howell et al.*, 2009]. In addition, heavy MYI originating in the Arctic Ocean may be imported into the waters of the NWP by advection through the Queen Elizabeth Islands (QEI) [*Howell et al.*, 2013]. That MYI ice is known to be some of the thickest sea ice in the world [*Melling*, 2002; *Haas et al.*, 2010], and together with its high mechanical strength [*Timco and Weeks*, 2010], presents the largest obstacle and hazard for transiting ships and offshore structures.

The observed decline of the Arctic's summer sea ice extent and thickness [*Meier et al.*, 2014], longer melt seasons in the CAA [*Howell et al.*, 2009], and future climate model projections have led to suggestions of a more navigable NWP by midcentury [*Sou and Flato*, 2009; *Smith and Stephenson*, 2013]. Caution should be taken with these suggestions because global climate models with their coarse resolution likely have difficulty capturing intricate sea ice dynamic processes within the narrow channels of the CAA. Specifically, the import, survival, and thickness of MYI are difficult to predict and may in fact increase during the transition to a sea ice-free Arctic with more mobile ice conditions in the QEI which are located between the Arctic Ocean and NWP [*Melling*, 2002; *Howell et al.*, 2013]. Presumably, MYI from the Arctic Ocean will be more heavily ridged and thicker [*Melling*, 2002; *Haas et al.*, 2010] than locally formed MYI, posing greater danger to transiting ships than locally grown MYI.

Apart from ice coverage and ice type, ice thickness is the most important sea ice property required to assess hazard potential and to initialize predictions of ice breakup, deformation, and melt [e.g., *Lindsay et al.*, 2012; *Smith and Stephenson*, 2013]. However, there is little information about ice thicknesses in the CAA. The only systematic study so far analyzed extensive drill-hole data taken in spring during the 1970s in the northern CAA [*Melling*, 2002]. Results showed mean late winter thicknesses of 3.4 m, with subregional means as large as 5.5 m. Those results may not be representative any more of current ice conditions. The Canadian Ice Service (CIS) publishes weekly charts of general ice conditions based on the analysis of various satellite

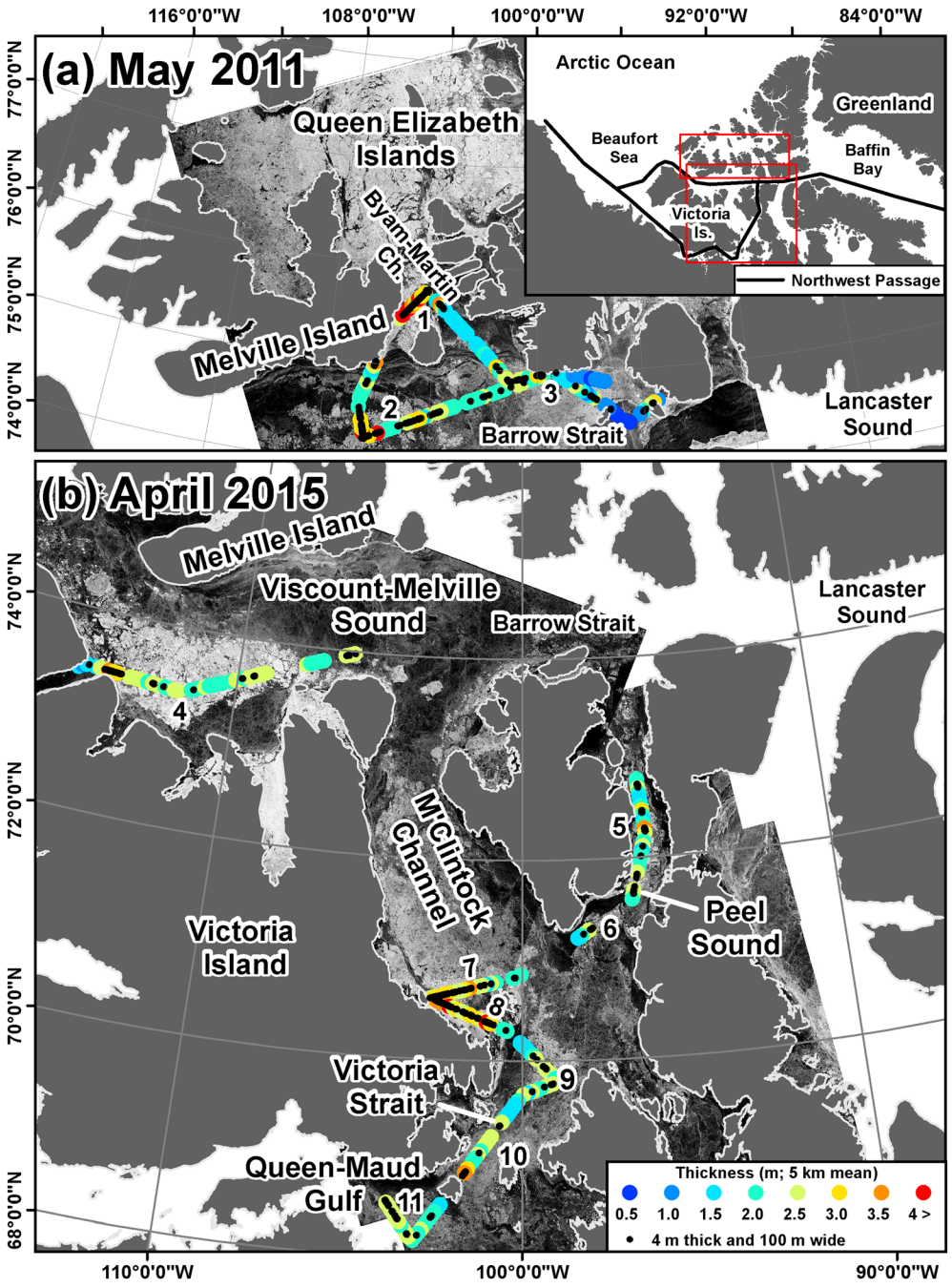

Figure 1. Maps of the Canadian Arctic Archipelago showing the two main routes of the Northwest Passage (inset), and tracks of airborne ice thickness surveys in (a) May 2011 and (b) April 2015 color coded by mean ice thickness of 5 km flight sections. Numbers along flight tracks correspond to specific regions analyzed in Figure 2 and Table 1, and black dots mark the locations of individual thick ice features thicker than 4 m and wider than 100 m. Background shows contemporary RADARSAT-2 images (radar backscatter σ_0) to demonstrate general distribution of multiyear ice (high σ_0, bright) and first-year ice (low σ_0), cf. with ice charts in Figures S1–S3. (RADARSAT-2 imagery © Canadian Space Agency).

imagery [*CIS*, 2006]. While their ice type and floe size information is quite accurate, they only provide a rough classification of ice thickness, with thickness classes of old FYI >1.2 m and old ice (2 to >3 m thick).

Here we present results of two airborne electromagnetic (AEM) ice thickness surveys performed in May 2011 and April 2015 over large parts of the NWP characterized by extensive coverage of MYI. These represent late winter ice conditions indicative of the maximum ice thickness reached in those two winters and are the first

ever large-scale assessment of ice thicknesses in the region in any season. Although most or all shipping activity does take place during the summer when the ice is mobile and has strongly thinned or completely melted out, late winter conditions are relevant for the prediction of ice breakup and melting potential, and it can be expected that thicker ice has a higher chance for surviving the summer melt and for posing marine hazards than thinner ice. In addition, the presence and thickness of MYI during the winter also represents ice conditions at the end of the previous summer when the same ice covered the region during the shipping season. Therefore, this study aims to (1) provide important baseline data for the evaluation of past and future ice thickness changes in the region, (2) present information for the development and initialization of forecast systems of the opening and navigability of the NWP, and (3) gather data for the assessment of the hazard potential for shipping in the NWP.

2. Methods and Measurements

Ice thickness surveys were carried out by means of airborne electromagnetic induction (AEM) sounding using a Bell 206 L helicopter in 2011 [*Haas et al*., 2009] and a DC3-T airplane in 2015 [*Haas et al*., 2010]. A map of the flight tracks is shown in Figure 1. On 16 May 2011, a 690 km long survey was performed over Barrow Strait, Viscount Melville Sound, and Byam-Martin Channel, requiring three refueling stops at fuel caches maintained by the Canadian Polar Continental Shelf Project. On 19 April 2015, 718 km of data were obtained in Peel Sound, M'Clintock Channel, Victoria Strait, and Queen Maud Gulf en route from Resolute Bay to Cambridge Bay. A 270 km long survey was conducted in Viscount Melville Sound on 25 April 2015, returning from Inuvik to Resolute Bay. Flight route planning had to consider variable and adverse weather conditions within these large regions. Therefore, it was impossible to include every relevant region of MYI in the surveys which may limit the representativeness of the presented results.

Surveys were performed with a tethered sensor package ("EM Bird") operated 20 to 80 m below the aircraft and 20 m above the ice. At aircraft speeds ranging between 90 and 120 knots, measurement point spacing ranged between 4.5 and 6 m.

The Bird's height above the ice/water interface is determined by means of electromagnetic induction in the conductive sea water, using a set of transmitting and receiving coils to generate and sense an alternating electromagnetic field with a frequency of 4060 Hz [*Haas et al*., 2009]. The Bird's altitude above the snow or ice surface is measured with a laser altimeter. Ice-plus-snow thickness (hereafter referred to as ice thickness) results from the difference between the electromagnetically determined altitude above the ice/water interface and the laser-measured altitude above the snow or ice surface.

Unfortunately, with AEM measurements it is not possible to distinguish between ice and snow thickness. In April/May, snow thickness ranges between 0.2 and 0.4 m in the study region [*Brown and Cote*, 1992; *Melling*, 2002]. Although snow thickness impacts thermodynamic ice growth [*Flato and Brown*, 1996], it is unlikely that the observed large thickness variability and deformation shown in this study are strongly affected by snow thickness variations.

In pack ice, there are occasional open leads with an ice thickness of 0 m which can be used for calibration of the ice thickness retrievals. Then the accuracy of EM measurements is ±0.1 m over level ice [*Pfaffling et al*., 2007; *Haas et al*., 2009]. However, over the fast ice in the CAA there are no open leads; and therefore, thickness retrievals can be more sensitive to slight uncertainties in drift and calibration [*Haas et al*., 2009]. Therefore, in the absence of any other thickness information useful for validation, we estimate the accuracy of the measurements presented here to be ± 0.15 m based on the instrument's internal consistency and the stability of electronic drift during calibration ascents to high altitudes [*Haas et al*., 2009].

However, AEM thickness retrievals underestimate the maximum thickness of pressure ridges due to their keel porosity and an EM footprint diameter of more than 45 to 60 m. The measured thickness of individual thick multiyear ridges can therefore be less than 24% of the "true" thickness [e.g., *Johnston and Haas*, 2011]. However, several studies have shown that regional, mean AEM ice thickness estimates tend to be similar or larger than retrievals from laser altimetry or upward looking sonar [e.g., *Lindsay et al*., 2012], likely due to the compensating effects of footprint averaging adjacent to ridge keels. Note that uncertainties of level ice thickness retrievals most strongly affect the accuracy of modal thicknesses, while uncertainties over ridges affect the magnitude and length of the tails of ice thickness distributions.

Ice thickness surveys were planned to connect regions of MYI, whose presence was inferred from a combination of CIS ice charts and RADARSAT-2 imagery. In order to provide historical background on the nature and origin of the surveyed ice, particularly the dominant multiyear ice regimes, series of historical ice charts and RADARSAT images were used to visually backtrack the ice over several seasons.

3. Results and Discussion

3.1. Mean Ice Thickness

The map in Figure 1 shows mean ice thickness in 5 km long flight sections overlaid on two coincident RADARSAT-2 images. In the RADARSAT-2 images, MYI can be identified by its higher backscatter (brighter pixels) and FYI by its lower backscatter (darker pixels), in general agreement with the CIS ice charts (Figures S1 and S3f in the supporting information). On this scale, most ice had mean thicknesses between 2 and 3 m. There were few regions where the ice was only 1 to 2 m thick or thinner. Those regions were characterized by younger FYI which had only formed later in the season in regions of previously local open water or coastal polynyas, most notably in Barrow Strait and Lancaster Sound in 2011. For example, western Lancaster Sound was only covered by mobile pack ice with open water and thin ice at its western end for most of the winters of 2011 and 2015. In addition, some regions may remain thinner throughout the winter due to the presence of strong under-ice currents which increase the local oceanic heat flux and thus retard ice growth [*Melling et al*., 2015].

The thickest ice of more than 3 m and up to 4 m mean thickness was found in the MYI regions of Byam-Martin Channel (BMC), Viscount Melville Sound (VMS), Peel Sound (PS), M'Clintock Channel (MCC), Victoria Strait (VS), and Queen Maud Gulf (QMG) (Figures 1, S1, and S3f). In 2011, the region of MYI in BMC and VMS originated in the Arctic Ocean and drifted through the QEI during the 2010 melt season.

In 2015, the MYI in VMS was primarily formed in situ. The CIS ice charts illustrate that the region was seasonal FYI before and at the peak of the melt season of 2014 (Figures S2a and S2b). A significant amount of this FYI survived the melt season and was promoted to second year ice (SYI) which is illustrated by the October 2014 CIS chart (Figure S3c, SYI shown in orange) and on the November RADARSAT-2 image (Figure S3d).

In contrast, all other MYI surveyed in and south of PS in 2015 was primarily Arctic Ocean MYI that slowly drifted through the CAA over several years. Figure S3a shows that the MCC was entirely FYI at the start of 2013 melt season. During the 2013 melt season, there was an appreciable southward flux of MYI that can be seen extending from the Arctic Ocean to the MCC (Figures S3b and S3c). A considerable amount of this MYI survived the 2013 melt season and eventually became landlocked in VMS/Barrow Strait and MCC (Figure S3d). In 2014, the remainder of the MYI in VMS gradually migrated southward and came to rest within the MCC, VS, and even farther south in the QMG. There was negligible additional MYI import from the QEI during the 2014 melt season because the ice arch in BMC, the primary exit channel for QEI MYI, did not break during the melt season. It is unclear if the ice in PS included traces of MYI from the QEI or was more regionally promoted SYI.

Mean ice thicknesses in BMC, VMS (2011), and MCC (Table 1) were larger than or within 0.2 m of the 3.4 m reported by *Melling* [2002] for ice farther north in the QEI during the 1970s. However, all this ice was much thinner than the contemporary, heavily deformed, Arctic Ocean MYI along the coast of Ellesmere Island which has mean thicknesses of more than 4 to 5 m [*Haas et al*., 2010]. Even though more of this ice can drift through the QEI in recent years [*Howell et al*., 2013], it seems to lose much of its mass during one or more summers of ablation and bottom melt [*Melling*, 2002].

3.2. Modal Ice Thickness

More insights can be gained from individual ice thickness distributions calculated for individual MYI and FYI regimes (Figure 2 and Table 1). These are characterized by one or several modes and long tails of variable amounts of deformed ice. Modal ice thicknesses ranged between 1.6 and 2.4 m, slightly less in 2011 than in 2015, with the majority of ice between 1.8 and 2 m thick. This is significantly thicker than the minimum thickness of 1.2 m indicated on the ice charts. Modal thicknesses are smaller than the 2.6 m reported by *Melling* [2002] for the QEI in the 1970s, in particular considering that our thicknesses include snow thickness. In light of this, our modal thicknesses are also some 0.2 to 0.4 m thinner than pre-1990s FYI thicknesses reported from nearshore shallow-water stations mostly farther north [*Brown and Cote*, 1992; *Flato and Brown*, 1996; *Melling*, 2002]. Given

Table 1. Ice Thickness Statistics for All Regions Surveyed in 2011 and 2015[a]

Year	Profile #; (Length, km)	Region[b]	Ice Type	Mode (m)	Mean[c] (m)	Q75 (m)	Mean25 (m)
2011	1 (37)	BMC	MYI	1.7	3.84 (2.03)	4.87	6.48
	2 (127)	VMS	MYI	1.8	3.21 (1.77)	3.90	5.64
	3 (242)	BS	FYI	1.6[d]	2.00 (1.18)	2.43	3.46
2015	4 (245)	VMS	SYI formed in situ	2.0	2.61 (0.81)	2.91	3.70
	5 (131)	PS	MYI	1.8	2.47 (1.04)	2.79	3.84
	6 (37)	PS	FYI	1.8	2.33 (0.87)	2.45	3.56
	7 (110)	MCC	MYI	2.0	2.78 (1.09)	3.21	4.22
	8 (45)	MCC	MYI	2.4	3.21 (1.15)	3.84	4.77
	9 (95)	VS	MYI	1.9	2.51 (0.77)	2.80	3.55
	10 (106)	VS	FYI	1.9	2.51 (1.00)	2.96	3.88
	11 (124)	QMG	MYI	2.0	2.48 (0.70)	2.75	3.44

[a]Q75 is 75% quartile, and Mean25 is the mean ice thickness of all measurements thicker than Q75. Cf. Figures 1 and 2 for locations and thickness distributions.
[b]See Figures 1 and 2.
[c]Mean (and standard deviation).
[d]Thickness distribution is bimodal with another mode at 0.9 m representing younger ice near the polynya in Lancaster Sound (see Figures 1 and 2).

the observed climate warming in the CAA of more than 2°C in the past 66 years [*Environment Canada*, 2014], one would expect thinner ice today than decades ago. However, without more in-depth modeling, the differences seem rather small and it is unclear how the results are also affected by a somewhat warmer climate in the lower latitudes of our study region and by the deeper channel regimes of our study regions with likely higher ocean heat fluxes than in nearshore bays.

It is remarkable that there was no clear difference of modal thicknesses of MYI, SYI, or FYI regimes in late winter. On the one hand, this may be due to the fact that the surveyed MYI regimes were derived from fields of MYI floes interspersed by open water in which FYI could form during the present winter. In fact, CIS ice charts showed fractions of between 10% and 40% FYI embedded in the MYI regimes in MCC and elsewhere, respectively. The impact may be seen when comparing the MYI and FYI thickness distributions in PS where the MYI distribution has a much broader shoulder of thicker ice than the FYI distribution (Figure 2, regions 5 and 6).

However, on the other hand, the similar modal thicknesses of 1.8 to 2.0 m could also imply that the ice is near its equilibrium thickness, where average conductive heat flux through the ice is balanced by ocean heat flux, such that no further net ice growth occurs, or where summer ablation is balanced by winter accretion [*Maykut and Untersteiner*, 1971]. Our results could thus imply that in the waters of the NWP equilibrium, thickness can be reached by FYI growth in one winter and will not be exceeded by SYI or MYI growth under the same freezing conditions. Assuming that level SYI or MYI floes have been thinner than the equilibrium thickness at the end of the previous summer, their finite thickness and possible snow coverage early in the freezing season could retard ice growth enough to be comparable to that of FYI [e.g., *Notz*, 2009]. We have made similar observations supported by drill-hole measurements farther north in the QEI in 2014 and 2015 (Haas and Mahoney, unpublished manuscript, 2015).

There were secondary modes of thinner ice in BMC (region 1), BS (region 3), and VS (regions 9 and 10), as shown in Figure 2. As explained above, these result from the presence of younger ice formed later in the winter in still active nearshore polynyas or from regions of enhanced ocean heat flux due to strong under-ice currents. Most notably, CIS ice charts showed that the narrowest part of VS maintained mobile ice conditions until the first week of February 2015, allowing formation of thin new ice in the northern parts and leading to strong deformation in the southern parts where the thicker ice was pushed against the neighboring stable fast ice.

3.3. Deformed Ice Thickness

The thickness distributions in Figure 2 show strong differences in the amount and thickness of deformed ice. The MYI in BMC and VMS in 2011 stands out for their very thick ice, as do the MYI regimes in MCC. To further distinguish between level and deformed ice and to possibly isolate the contributions of MYI to the thickest classes of the ice thickness distributions, we have computed 75% quartiles and the mean thickness of the thickest 25% of all measurements in each region (Figure 2 and Table 1). Again, the ice in BMC and VMS in

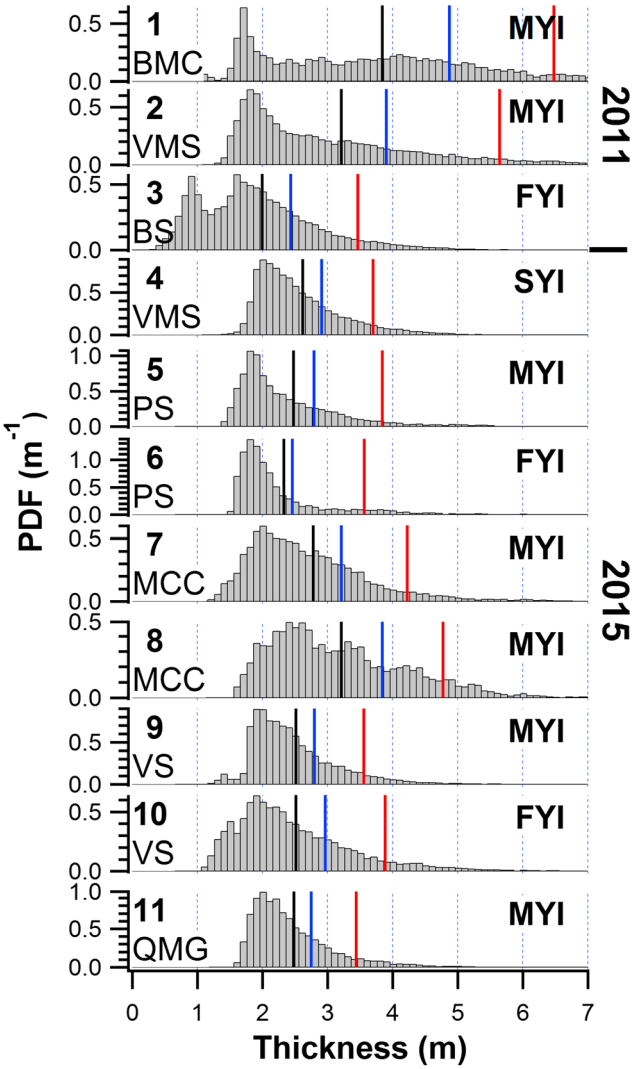

Figure 2. Ice thickness distributions (probability density functions) of all regions surveyed in 2011 and 2015, from north to south. Region numbers refer to numbers in Figure 1 and Table 1. Black, red, and blue vertical lines show mean ice thickness, 75% quartile, and mean thickness of thickest 25% of data, respectively (cf. Table 1). BMC: Byam-Martin Channel; VMS: Viscount Melville Sound; BS: Barrow Strait; PS: Peel Sound; MCC: M'Clintock Channel; VS: Victoria Strait; and QMG: Queen Maud Gulf.

2011 stands out with 75% quartiles of more than 3.9 m, closely followed by the MYI in MCC. Although these values are significantly smaller than the 5.42 m 75% quartile reported by *Melling* [2002] for the QEI in the 1970s, they show that BMC and the QEI are still the source of very thick MYI today. The MYI observed in MCC was derived from this region and with 75% quartiles of $>=3.21$ m was the thickest ice south of BS, while the 75% quartile of SYI in VMS in 2015 was almost a meter less than that of the MYI in the same region in 2011.

Overall, there is a tendency for the deformed ice to get thinner with decreasing northern latitude, continuing the trends discussed above when drifting through the QEI. For example, the deformed ice properties become thinner from MCC to the south, and the ice in QMG has the smallest deformed ice statistics (Table 1). As proposed by *Melling* [2002], this may be a result of longer residence time in more open ice conditions while drifting south during summers which will lead to more lateral melt and erosion of ridged ice.

The thickness distributions bear no information about the spatial relationship between measurements of thick ice. To identify the thickest and most severe ice including multiyear hummock fields, and to distinguish it from more confined pressure ridges, we have analyzed the occurrence of thick ice features which are at least 4 m thick over distances of at least 100 m. This scale was chosen because it is comparable to the typical length of ships traveling the region, and such ice more than 4 m thick would certainly stop a transit. One hundred eighty-seven such features were found in 2011, and 197 in 2015, 36 in VMS, and 161 between PS and QMG. Locations of thick ice features are shown in Figure 1 and are variable along the flight tracks, with larger spatial densities in the thicker MYI regions. On average, numbers correspond to average spatial densities of thick ice features of 0.23 km^{-1}, 0.13 km^{-1}, and 0.22 km^{-1}, respectively. The mean lengths and thicknesses of thick ice features were 231 m and 5.66 m, 162 m and 5.25 m, and 209 m and 5.46 m, respectively, i.e., were the most severe in 2011, followed by the MCC survey in 2015.

If we assume that the thermodynamic equilibrium thickness of sea ice in the NWP is approximately 2 m (see above), then it follows that those thick ice features, as well as any level ice thicker than 2 m observed here, will likely have been as thick or even thicker in the previous summer as well. It is more difficult to make such statement for deformed ice, because in addition to ridges surviving the previous summer there is a lot of deformation taking place in fall before the ice cover finally consolidates and becomes landfast.

4. Conclusions

We have presented snow-plus-ice thickness observations from major parts of the NWP obtained in late winter of 2011 and 2015 with a focus on regions of MYI coverage. The origin and type of MYI were reconstructed based on series of CIS ice charts and RADARSAT-2 images. Results show that most regions had modal thicknesses ranging between 1.8 and 2.0 m. Mean thicknesses ranged between 2 and 3 m. However, MYI in Byam-Martin Channel and MYI in Viscount Melville Sound and M'Clintock Channel originating from there was thicker than 3 m on average.

There was large regional variability in mean thicknesses and in the thickness and amount of deformed ice. This can mostly be explained by differences in FYI age, snow cover, ocean heat flux, local deformation of FYI, and by the origin of MYI and its residence time in the waters of the NWP during previous summers. Accordingly, ice thicknesses and the amount of thick, deformed ice decrease toward the south.

There are no data with which we could easily compare our results to evaluate possible thickness changes and an easing of ice conditions for marine operations in the NWP. For further evaluation, it is also important to consider that in Parry Channel, including VMS, i.e., in the waters of the northern NWP, in 2014 more ice survived the summer as MYI than in the nine most recent years but slightly less than during 1968–2015 on average (Figure S5). Between November 2014 and April 2015, winter air temperatures were between −0.5°C and −1.5°C colder than during 1980–2010 which could have led to slightly thicker level ice than average, notwithstanding snow effects (Figure S4). Our results show that modal thicknesses were 0.4 to 0.6 m less than observed prior to the 1990s in regions farther north [*Brown and Cote*, 1992; *Melling*, 2002], with reductions in deformed ice thickness more difficult to judge. This apparent thinning could be a direct consequence of the observed climate warming in the CAA. However, by all means the observed thicknesses and amount of deformed ice still indicate serious ice conditions which can persist throughout the summers and provide ample potential for encounters with hazardous ice. Even in recent years, the CAA remains a source for locally grown MYI and a sink for Arctic Ocean MYI [*Howell et al.*, 2015]; and therefore, shipping through the NWP should not be taken lightly. These conclusions also support results of *Smith and Stephenson* [2013] who suggested that the NWP will not become easily navigable for another 40 years or so.

We have also shown that there are large numbers of thick ice features with thicknesses of more than 4 m over distances of more than 100 m which have the largest probability to survive through the summer. In addition, we have observed two ice islands in and south of Byam-Martin Channel in 2011 which were not included in the present analysis. These ice islands originated from the ice shelves along the Arctic Ocean coast of Ellesmere Island, and were between 30 and 40 m thick, adding to the variability of hazardous ice features in the NWP.

In winter and spring, AEM thickness surveys provide the best means to collect accurate, near-real-time ice thickness data from the vast expanses of the NWP to observe ice thickness change in the region and to collect information for the initialization of models predicting ice breakup and decay for better planning of the shipping season. Even though in winter their accuracy is somewhat reduced due to the absence of open water, they are less affected than, e.g., laser or radar altimeter measurements, which rely on the presence of open water as reference tie points for their freeboard retrievals. However, at present, no program exists to collect such data in any season or in any systematic or routine way.

Despite the importance of sea ice thickness for forecasting ice conditions and hazard potential, we note that knowledge of other ice properties like ice concentration, floe size, ice drift, and ice pressure during the shipping season is also important for an information and prediction system for economic and safe shipping in the NWP.

Acknowledgments

The development and installation of surveying equipment, performance of surveys, and data analysis were conducted with funds from Alberta Ingenuity (AI), Canadian Foundation for Innovation (CFI), Natural Sciences and Engineering Research Council (NSERC) Discovery Grant (DG) and Canada Research Chair (CRC) programs, Beaufort Regional Environmental Assessment (BREA), Marine Environmental Observation, Prediction, and Response Network (MEOPAR), and ArcticNet. In addition, support by the Polar Continental Shelf Program (PCSP) is gratefully acknowledged. We thank Anne Bublitz (York University) for her invaluable help with the 2015 surveys and pilots Jim Haffey (Kenn Borek Air) and Gerry Nuttal (Universal Helicopters NL) and their crews. Comments by Garry Timco and another reviewer are much appreciated. Supporting data are included as SI and Data Sets S1–S3.

The Editor thanks two anonymous reviewers for their assistance in evaluating this paper.

References

Brown, R. D., and P. Cote (1992), Interannual variability of land-fast ice thickness in the Canadian High Arctic, 1950–89, *Arctic*, *45*, 273–284.

CIS (2006), *Canadian Ice Service Digital Archive—Regional Charts: History, Accuracy, and Caveats*, *CIS Arch. Doc. Ser.*, vol. 1, Canadian Ice Service, Ottawa, Canada. [Available at http://ice.ec.gc.ca/IA_DOC/cisads_no_001_e.pdf.]

Environment Canada (2014), Climate trends and variations bulletin—Annual 2014. [Available at http://www.ec.gc.ca/adsc-cmda/default.asp?lang=En&n=188031DB-1, Accessed Aug. 3, 2015.]

Flato, G. M., and R. D. Brown (1996), Variability and climate sensitivity of landfast Arctic sea ice, *J. Geophys. Res.*, *101*, 25,767–25,778, doi:10.1029/96JC02431.

Haas, C., J. Lobach, S. Hendricks, L. Rabenstein, and A. Pfaffling (2009), Helicopter-borne measurements of sea ice thickness, using a small and lightweight, digital EM system, *J. Appl. Geophys.*, *67*(3), 234–241, doi:10.1016/j.jappgeo.2008.05.005.

Haas, C., S. Hendricks, H. Eicken, and A. Herber (2010), Synoptic airborne thickness surveys reveal state of Arctic sea ice cover, *Geophys. Res. Lett.*, *37*, L09501, doi:10.1029/2010GL042652.

Howell, S. E. L., C. R. Duguay, and T. Markus (2009), Sea ice conditions and melt season duration variability within the Canadian Arctic Archipelago: 1979–2008, *Geophys. Res. Lett.*, *36*, L10502, doi:10.1029/2009GL037681.

Howell, S. E. L., T. Wohlleben, M. Dabboor, C. Derksen, A. Komarov, and L. Pizzolato (2013), Recent changes in the exchange of sea ice between the Arctic Ocean and the Canadian Arctic Archipelago, *J. Geophys. Res. Oceans*, *118*, 3595–3607, doi:10.1002/jgrc.20265.

Howell, S. E. L., C. Derksen, L. Pizzolato, and M. Brady (2015), Multiyear ice replenishment in the Canadian Arctic Archipelago: 1997–2013, *J. Geophys. Res. Oceans*, *120*, 1623–1637, doi:10.1002/2015JC010696.

Johnston, M., and C. Haas (2011), Validating helicopter-based EM (HEM) thicknesses over very thick multi-year ice, *Proceedings 21st Conference on Port and Ocean Engineering under Arctic Conditions (POAC'11)*, Pap. POAC11-132, Montreal, Canada, July 10-14, 2011, ISSN 2077-7841, 11 pp.

Lindsay, R., C. Haas, S. Hendricks, P. Hunkeler, N. Kurtz, J. Paden, B. Panzer, J. Sonntag, J. Yungel, and J. Zhang (2012), Seasonal forecasts of Arctic sea ice initialized with observations of ice thickness, *Geophys. Res. Lett.*, *39*, L21502, doi:10.1029/2012GL053576.

Maykut, G. A., and N. Untersteiner (1971), Some results from a time-dependent thermodynamic model of sea ice, *J. Geophys. Res.*, *76*(6), 1550–1575, doi:10.1029/JC076i006p01550.

Meier, W. N., et al. (2014), Arctic sea ice in transformation: A review of recent observed changes and impacts on biology and human activity, *Rev. Geophys.*, *52*, 185–217, doi:10.1002/2013RG000431.

Melling, H. (2002), Sea ice of the northern Canadian Arctic Archipelago, *J. Geophys. Res.*, *107*(C11), 3181, doi:10.1029/2001JC001102.

Melling, H., C. Haas, and E. Brossier (2015), Invisible polynyas: Modulation of fast ice thickness by ocean heat flux on the Canadian polar shelf, *J. Geophys. Res. Oceans*, *120*, 777–795, doi:10.1002/2014JC010404.

Notz, D. (2009), The future of ice sheets and sea ice: Between reversible retreat and unstoppable loss, *Proc. Natl. Acad. Sci. U.S.A.*, *106*(49), 20,590–20,595, doi:10.1073/pnas.0902356106.

Pfaffling, A., C. Haas, and J. E. Reid (2007), A direct helicopter EM sea ice thickness inversion, assessed with synthetic and field data, *Geophysics*, *72*, F127–F137.

Smith, L. C., and S. R. Stephenson (2013), New Trans-Arctic shipping routes navigable by mid-century, *Proc. Natl. Acad. Sci. U.S.A.*, *110*(13), E1191–E1195, doi:10.1073/pnas.1214212110.

Sou, T., and G. Flato (2009), Sea ice in the Canadian Arctic Archipelago: Modeling the past (1950-2004) and the future (2041-60), *J. Clim.*, *22*, 2181–2198, doi:10.1175/2008JCLI2335.1.

Timco, G. W., and W. F. Weeks (2010), A review of the engineering properties of sea ice, *Cold Reg. Sci. Technol.*, *60*, 107–129.